Received February 18, 2020, accepted February 29, 2020, date of publication March 6, 2020, date of current version March 17, 2020.

Digital Object Identifier 10.1109/ACCESS.2020.2978904

Task Scheduling for Multi-Target ISAR Imaging in Radar Network

DAN WANG[1,2], QUN ZHANG[1,2], (Senior Member, IEEE), YING LUO[1,2], (Member, IEEE), KAI-MING LI[1,2], AND XIAO-WEN LIU[3]

[1]Institute of Information and Navigation, Air Force Engineering University, Xi'an 710077, China
[2]Collaborative Innovation Center of Information Sensing and Understanding, Xi'an 710077, China
[3]School of Information and Communications, National University of Defense Technology, Xi'an 710100, China

Corresponding author: Qun Zhang (zhangqunnus@gmail.com)

This work was supported in part by the National Natural Science Foundation of China under Grant 61631019, Grant 61801516, Grant 61701530, and Grant 61871396.

ABSTRACT For radar imaging of multiple targets in radar network, it is necessary to schedule the imaging tasks among various radars at suitable time to achieve high performance under limited radar resources. In this paper, based on the image quality requirement, a task schedule method is proposed for multi-target inverse synthetic aperture radar (ISAR) imaging in radar network. Due to the image resolution is an important indicator of image quality and the imaging task is time sensitive, the relationship between the imaging resolution and task time is studied firstly. Thereafter, the task scheduling problem is converted into an optimization problem with time window constrains and an improved Quantum Genetic Algorithm (IQGA) is proposed to solve the problem. Then the task scheduling strategy which contains how to allocate the targets to the radars and when to observe the targets can be obtained. Finally, simulation results verify the effectiveness of the proposed method. With the help of the propose method, the multi-target ISAR task can be completed effectively and the resource utilization of the radar network can be improved.

INDEX TERMS Radar network, multi-target imaging, task scheduling optimization, time window, improved quantum genetic algorithm (IQGA).

I. INTRODUCTION

Recent years, high resolution ISAR imaging techniques have been widely used in military and civil fields such as target classification, field surveillance and human behavior understanding due to its all-day and all-weather surveillance capability [1]. An ISAR image is a 2-D projection of the target on the range-Doppler plane with the direction of range and direction of gradient of Doppler frequencies [2]. For a mono-static radar, when the target is moving along the radar line of sight, the viewing angle does not change with time and hence the ISAR image cannot be produced [2]. Compared with a mono-static radar, the radar network has many advantages. For instance, when the target is observed by the radar network, the observation data from different angles can be obtained simultaneously and the ISAR image can be produced effectively [3]. Moreover, combined with the multi-angle information, the radar network can improve the performance of information acquisition, avoiding blind velocities, anti-interference and anti-destruction [4].

A radar network can simultaneously perform multiple tasks such as the target searching, tracking, imaging and recognition, etc. In the face of the increasingly complicated electromagnetic environment, it is unlikely for one mono-static radar to complete all the tasks. Multiple targets and multiple tasks should be completed by radar network, while the radar resource is extremely valuable and limited. For instance, it usually takes a long observation time to obtain an ISAR image with expected image quality while the resource assigned to one single task is limited especially when a lot of targets need to be reconnoitered and imaged. Thus, reasonable and effective radar resource allocation algorithms are important and essential [5]–[19].

Recently, a lot of published researches have been conducted on the radar network. Yang *et al.* proposed a joint antenna placement and transmitted power allocation algorithm for improving the surveillance performance of the distributed radar network [6]. Zhang *et al.* proposed an optimal

The associate editor coordinating the review of this manuscript and approving it for publication was Ravibabu Mulaveesala.

antenna deployment algorithm to solve the problem of multiple regions for interference simultaneously and the simulation results are provided to demonstrate the effectiveness of the proposed algorithm [7]. Yan *et al.* proposed a joint threshold adjustment and power allocation algorithm for target tracking in asynchronous radar network [8]. Furthermore, Tian *et al.* proposed a timeliness constrained task scheduling algorithm to solve the multifunction radar network task scheduling problem and the numerical results verify the validity of the proposed task scheduling algorithm [9]. However, these studies focus on the multi-target detection, tracking, location scheme, estimation of the target characteristics, while there are few researches on the optimization of imaging task scheduling problem in radar network. In [14], for the first time, a multi-target imaging task allocation method in radar network has been proposed in our previous work, in which the relaxed convex optimization theory is used to solve the imaging task allocation problem. In order to further study the multi-target imaging task scheduling problem in radar network, we try to use other theories to solve the task scheduling problem in this paper.

In this paper, we propose a task scheduling strategy of multi-target ISAR imaging task for the radar network. For an ISAR task, imaging quality should be considered at first and the imaging resolution is an important indicator of imaging quality. When using conventional range-Doppler (RD) algorithm to conduct the ISAR image, the relationship between the imaging resolution and task time can be analyzed. Then the task scheduling problem can be converted into an optimization problem with time window constrains. The optimization problem with time window is a complex process, which includes task allocation and imaging time selection. Thereafter, an improved Quantum Genetic Algorithm (IQGA) is proposed to solve the problem. With the help of the proposed method, the task scheduling for multi-target ISAR imaging in radar network can be completed effectively, and the resource utilization of the radar network can be improved while imaging quality requirement is fulfilled.

The paper is organized as follows. The multi-target task scheduling model of the radar network is constructed in Section II. In Section III, an improved Quantum Genetic Algorithm (IQGA) is proposed to solve the optimization problem. Simulation results and analysis are presented in Section IV. Finally, conclusion is drawn in Section V.

II. PROBLEM FORMULATION

A. SYSTEM MODEL OF RADAR NETWORK

As shown in Fig.1, we consider that the multi-target scene consisting of a set of radars $R = \{r_1, r_2, \cdots, r_M\}$ and a set of targets $D = \{d_1, d_2, \cdots, d_N\}$ where M and N are the numbers of radars and targets respectively. In general, the number of the targets is greater than the number of radars. Multiple radars are independently distributed at different spatial positions in a radar network. For the sake of simplicity, for imaging task, each target can only be allocated to one radar and each radar can only illuminate one target at one time.

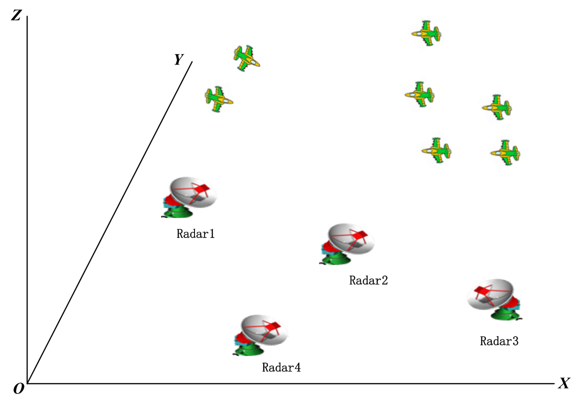

FIGURE 1. The multi-target imaging scene in the radar network.

In practice, it usually takes a long continuous observation time to obtain an ISAR image with expected image quality while the resource assigned to one single task is limited especially when a lot of targets need to be reconnoitered and imaged. In the case multiple targets appear in the imaging area and a target can be imaged independently by different radars, the selection of radar to image a suitable target at a suitable time is important. The scheduling scheme not only affects the total imaging task time, but also affects resource utilization of the radar network. Hence it is necessary to construct a task scheduling optimization model to improve the radar resource utilization.

For the ISAR imaging task, image quality is an important factor to be considered and image resolution is usually chosen to evaluate the ISAR image quality. As a matter of fact, different targets with different radar cross section (RCS) may require different resolutions. Hence, it is necessary to conduct some analysis on the imaging time with respect to the image resolution requirement.

B. IMAGING TIME UNDER REQUIRED IMAGE QUALITY

For an ISAR imaging task, the image quality is often selected as the quality indicator. As is known to all an ISAR image quality often depends on the range and azimuth resolution. Then it is essential to conduct some analysis on the relationship between the imaging time with the range and azimuth resolution.

It is well known that the range resolution is mainly determined by the transmitted signal bandwidth, which can be described by

$$\rho_r = c/2B \tag{1}$$

where c is the wave propagation velocity, B is the transmitted signal bandwidth. Obviously the range resolution is inversely proportional to the bandwidth. When higher range resolution requires, the bandwidth should become larger.

According to the radar equation [1], the maximum radar range $R_{\max}$ can be calculated as

$$R_{\max} = \left[\frac{P_t G^2 \lambda^2 \sigma}{(4\pi)^3 k T_0 B F_n (\frac{S}{N})_{o\ \min}}\right]^{1/4} \tag{2}$$

where P_t is the radar transmitted power, G is the antenna gain, λ is the wavelength of the transmitted signal, σ is the RCS of the target, k is the Boltzmann's constant, T_0 is the standard temperature (290K), and F_n is the noise figure of the receiver. The value of signal to noise ratio $(S/N)_{omin}$ is that required if only one pulse is present.

According to (2), it is obviously that the bandwidth is inversely proportional to the fourth power of the maximum radar range. Therefore, when larger bandwidth requires, the maximum radar range becomes smaller, so that the target takes much more time to fly into the imaging area to meet the required resolution as illustrated in Fig.2.

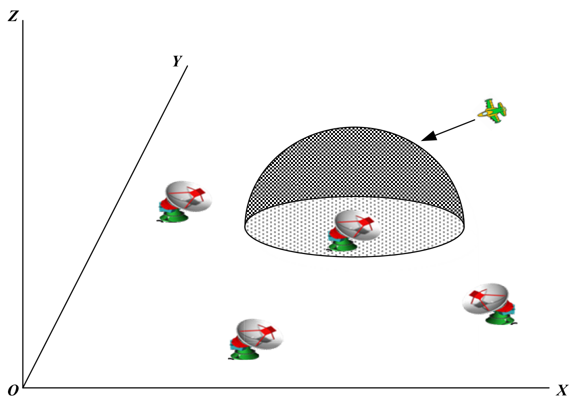

FIGURE 2. **The radar imaging area determined by the radar maximum range.**

Fig.2 shows the radar imaging area as the grid area by the radar maximum. In other words, only the target fly into the imaging area, the required range resolution can be met. When the radar bandwidth is calculated according to the required range resolution by (1), the maximum radar range can be calculated by the radar equation (2). Thereafter the imaging area of different radars and targets can be determined. Then the imaging time window which means the imaging task should start and finish within it can be obtained according to the imaging area and the speed of the target.

Suppose the three-dimensional spatial coordinates of the n-th target, m-th radar at the initial time be (x_n, y_n, z_n), (x_m, y_m, z_m) respectively. Then the spatial coordinates of the n-th target $\left(x_n', y_n', z_n'\right)$ at any time t can be determined by

$$\begin{aligned} x_n' &= x_n + v_x \cdot t \\ y_n' &= y_n + v_y \cdot t \\ z_n' &= z_n + v_z \cdot t \end{aligned} \tag{3}$$

where the speed vector of the n-th target is $\mathbf{V}_n = \left(v_x, v_y, v_z\right)$.

Let $R_{\max}^{mn}$ denotes the maximum radar range of the m-th radar for the n-th target, $R_{\max}^{mn}$ satisfies as

$$\sqrt{\left(x_l' - x_m\right)^2 + \left(y_l' - y_m\right)^2 + \left(z_l' - z_m\right)^2} \le R_{\max}^{mn} \tag{4}$$

Therefore the time window of the imaging task $[t_s^{mn}, t_e^{mn}]$ can be calculated by the combination of (3) and (4), where the time t_s^{mn} and t_e^{mn} denotes the moment the target first fly into the imaging area and the time the target fly out the imaging area respectively. Then the imaging start time of the imaging task t_i should be within the time window and the imaging task should be finish within the time window, otherwise the imaging task may not be performed.

Also, when using the Fourier transform to do the Doppler analysis, the azimuth resolution ρ_a is mainly determined by the rotation angle θ, which can be described as

$$\rho_a = \lambda / 2\theta \tag{5}$$

Obviously, the azimuth resolution in the radar imaging is inversely proportional to the rotation angle. When higher azimuth resolution requires, the rotation angle should become larger. Furthermore, the larger the rotation angle is, the longer the synthetic aperture time is. Therefore, the synthetic aperture time (i.e., the imaging time) is connected with the azimuth resolution.

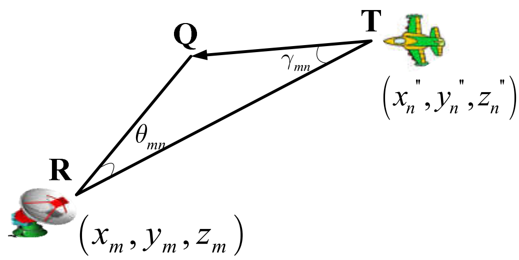

FIGURE 3. **Initial scenario of imaging process.**

Fig.3 shows the geometric diagram of the imaging process. The point R represents the position of the m-th radar, while the point T represents the position of the target at the imaging start moment and its spatial coordinates $\left(x_n'', y_n'', z_n''\right)$ can be determined by

$$\begin{aligned} x_n'' &= x_n + v_x \cdot t_i \\ y_n'' &= y_n + v_y \cdot t_i \\ z_n'' &= z_n + v_z \cdot t_i \end{aligned} \tag{6}$$

The point Q represents the position of the target at the imaging terminal moment. According to the knowledge of ISAR, the line TQ is the synthetic aperture length and the direction of line TQ from the point T to the point Q is identical to the flight direction of the target. According to the geometrical relationship in Fig.3 and the speed vector $\mathbf{V}_n$, the angle γ_{mn} can be determined by

$$\gamma_{mn} = \arccos\left(\frac{\boldsymbol{R}_{mn} \cdot \boldsymbol{V}_n}{|\boldsymbol{R}_{mn}| \cdot |\boldsymbol{V}_n|}\right) \tag{7}$$

where $\boldsymbol{R}_{mn} = \left(x_n'' - x_m, y_n'' - y_m, z_n'' - z_m\right)$ is the distance vector from the point T to the point R.

Therefore, according to the geometrical relationship, the synthetic aperture length and the synthetic aperture time with respect to the m-th radar and the n-th target can be determined by

$$L_{mn} = \frac{|\boldsymbol{R}_{mn}| \cdot \sin\theta_{mn}}{\sin(\gamma_{mn} + \theta_{mn})} \tag{8}$$

$$T_{amn} = L_{mn}/|\boldsymbol{V}_n| = \frac{|\boldsymbol{R}_{mn}| \cdot \sin\theta_{mn}}{\sin(\gamma_{mn} + \theta_{mn}) \cdot |\mathbf{V}_n|} \tag{9}$$

The synthetic aperture time T_{amn} is exactly the imaging time. Therefore, the imaging time is determined by the rotation angle and the geometry position of the target and the radar at the imaging start moment. Once the he geometry position of the target and the radar is different, the imaging time may be different. Thus, the imaging task is time sensitive that if imaging start moment is different, the imaging time is different. In a case when the azimuth resolution is given and the imaging start moment is chosen, the rotation angle can be calculated by (5), the imaging time can be obtained by (9).

As a matter of fact, the smaller the imaging time is, the more tasks can be performed, the higher the radar resource utilization in the radar network is. Therefore, the suitable imaging start time is necessary and essential to be analyzed.

According to the above analysis, to improve the radar resource utilization under the image quality requirement, the selection of the imaging start time is also necessary and the imaging task should be fulfilled within the time window constrains.

Therefore, how to allocate the targets to the distributed radars and when to observe the targets will affect the radar resource utilization, and deserved to be further analyzed.

C. TASK SCHEDULING MODEL

According to the above analysis, the imaging time is time sensitive and the imaging start time of the target should be selected within a continue time window. Therefore the task scheduling optimization model can be constructed with time window constrains. Compared with the general task scheduling problem, in this paper the selection of the imaging start time are also taken into consideration that make the problem more complicated.

Let $V_i = \{W_{i,1}, \cdots, W_{i,k}, \cdots, W_{i,M}\}$ denotes the imaging time window of the i-th target. Due to the relative positions of the target and each radar are different, the imaging time windows of the same target observed by different radar are different. $W_{i,k} = \{t_s^{i,k}, t_e^{i,k}\}$ represents the k-th imaging time window of the i-th task; $t_s^{i,k}, t_e^{i,k}$ are the start time and terminal time of the imaging time window respectively. An imaging task should start and finish within the selected time window.

Hence, the imaging task scheduling problem can be described as: given the set of available radars and tasks, each task has multiple time windows to be chosen through preprocessing. The task scheduling strategy is to select a set of tasks to be observed from the task set on the premise of satisfying the constraints. Then select a time window for these selected tasks from their time window set, and select the imaging start time for the selected tasks. So, in this paper, task selection, time window selection and imaging start time selection are adopted to describe the decision-making in the task scheduling.

The scheduling goal is to maximize the resources utilization of the radar network. On this basis, two performance metrics are used to evaluate the resources utilization.

(1) The sum of the priority of the selected tasks (SPI), defined by

$$SPI = \sum_{i=1}^{N} x_i P_i \tag{10}$$

where P_i represents the priority of the i-th target, and x_i represents the task decision variable contains only 0 and 1. The element 1 and 0 (i.e., $x_i = 1$ and $x_i = 0$) represent whether the i-th target is selected to be imaged or not.

(2) Resource surplus rate (RSR) of the radar network, defined by

$$RSR = 1 - \sum_{i=1}^{N} x_i T_{ai}/T_c \tag{11}$$

where T_{ai} is the imaging time of the i-th target and T_c is the total scheduling time. The bigger the resource surplus rate, the less the radar resources are used for multi-target imaging task while the imaging tasks are performed.

During the task scheduling, all radars $r_m \in R$ pursuit maximizing their own revenue, that is maximizing the SPI and RSR to improve the radar resource utilization.

In view of the above analysis, the task scheduling model for multi-target ISAR imaging can be formulated as

$$\begin{aligned} &\max(\omega_1 \cdot SPI + \omega_2 \cdot RSR) \\ &s.t. \begin{cases} x_i \in \{0, 1\} \\ y_i \in \{1, \cdots, M\} \\ \quad t_s^{i,y_i} \le t_i \le t_e^{i,y_i} \\ t_s^{i,y_i} \le t_i + T_{ai} \le t_e^{i,y_i} \\ t_i + T_{ai} \le t_j, \text{if } y_i = y_j \end{cases} \end{aligned} \tag{12}$$

where w_1 and w_2 are the adjustment factors representing impact degree of different performance metrics on the scheduling model. y_i represents the decision variable of time window selection, while $y_i = k$ represents the time window $W_{i,k}$ is selected to perform the imaging task of the i-th target. t_i represents the decision variable of imaging start time selection and T_{ai} represents the imaging time of the i-th target. The imaging start time and imaging terminal time should be within the selected time window. For the targets allocated to the same radar, the imaging start time of the latter target cannot be earlier than the terminal time of the previous target.

Obviously, the task scheduling problem is a multi-variable problem with time window constraints. Binary, integer and real number decisions are used to describe the task selection, time window selection, and imaging start time selection respectively. Therefore the task scheduling problem is an optimization problem that two discrete variables and one continuous variable coexist.

Compared with the general task scheduling model, by separately describing task selection, time window selection, and imaging start time selection, the imaging task scheduling problem is better described by the proposed model.

III. TASK SCHEDULING ALGORITHM DESIGN

On the basis of the above analysis, the task scheduling problem is a multi-variable optimization problem involving discrete variables continuous variable. There is no doubt the task scheduling problem is a complicated and an NP hard problem. Therefore, an optimization algorithm is necessary to be investigated in order to solve the problem.

In terms of optimization algorithms, existing research mostly focus on intelligent optimization algorithms and heuristic algorithms, such as genetic algorithm (GA), particle swarm optimization (PSO) and ant colony algorithms (ACO). These algorithms are used to solve the discrete optimization problem or the continuous optimization problem. However, the binary decision variable x_i, the integer decision variable y_i and the real number variable t_i coexist in the proposed model make the problem much more complicated that traditional task scheduling algorithms can't effectively adapt to the problem. So an improved Quantum Genetic Algorithm (IQGA) is proposed based on hybrid coding of binary and real numbers to solve the optimization problems with discrete and continuous decision variables. We will first briefly introduce the traditional Quantum Genetic Algorithm, and then expatiate the proposed improved Quantum Genetic Algorithm in detail.

A. QUANTUM GENETIC ALGORITHM

The Genetic Algorithm (GA) [20]–[28] is an efficient search and optimization method that automatically acquires and accumulates knowledge about the discrete search space, and adaptively controls the search process to find the best solution. But the convergence speed is slow, and it is easy to be limited to the local optimal.

In the quantum informatics, the carrier of the information is no longer a classical bit, but a quantum system with two states. The system can be an atom with two energy levels, or a photon with two polarizes directions, which is called the quantum bit or qubit [20]. Other than the classical bit, a quantum bit can be in any superposition of two ground states '0' and '1', which is called the quantum superposition.

Based on the concepts of qubits and the quantum superposition, Han proposed a quantum genetic algorithm (QGA) combined with genetic algorithm [20].

In the quantum genetic algorithm, a qubit may be in the '1' sate, in the '0' state, or in any superposition of the two. The state of a qubit can be represented as

$$|\Psi\rangle = \alpha |0\rangle + \beta |1\rangle \tag{13}$$

where α and β are complex numbers that specify the probability amplitudes of the corresponding states and satisfy the equation $|\alpha|^2 + |\beta|^2 = 1$ and $|\beta|^2$ denotes the probability that the qubit will be found in state '0' and state '1' respectively.

In QGA, the chromosome which represents a possible solution to the problem to be solved is a string of qubits. A chromosome with m qubits can be represented as

$$q = \begin{pmatrix} \alpha_1 & \alpha_2 & \cdots & \alpha_m \\ \beta_1 & \beta_2 & \cdots & \beta_m \end{pmatrix} \tag{14}$$

where $|\alpha_i|^2 + |\beta_i|^2 = 1, i = 1, 2, \ldots, m$.

For example, a three-qubit chromosome with three pairs of amplitudes such as

$$\begin{pmatrix} 1/\sqrt{2} & 1/2 & 1/\sqrt{2} \\ 1/\sqrt{2} & \sqrt{3}/2 & -1/\sqrt{2} \end{pmatrix}$$

Then the states can be presented as

$$\frac{1}{4}|000\rangle - \frac{1}{4}|001\rangle + \frac{\sqrt{3}}{4}|010\rangle - \frac{\sqrt{3}}{4}|011\rangle + \frac{1}{4}|100\rangle - \frac{1}{4}|101\rangle + \frac{\sqrt{3}}{4}|110\rangle - \frac{\sqrt{3}}{4}|111\rangle$$

The above result means that the probabilities to represent the states $|000\rangle$, $|001\rangle$, $|010\rangle$, $|011\rangle$, $|100\rangle$, $|101\rangle$, $|110\rangle$ and $|111\rangle$ are 1/16, 1/16, 3/16, 3/16, 1/16, 1/16, 3/16, and 3/16, respectively. Therefore, the above three-qubit string contains the information of eight states at the same time.

As quantum system can describe superposition states, a quantum chromosome can describe much more states and the quantum genetic algorithm has a better characteristic of population diversity than traditional algorithms.

Unlike GA's reproduction by the means of selection, crossover and mutation, in the QGA parent generations create the next generation through the rotation operation based on quantum-gate which is designed to make individuals to mutate in the direction of the better individual in current generation.

In particular, a rotation gate $U(\theta)$ is employed to update a quantum individual as

$$\begin{bmatrix} \alpha_i' \\ \beta_i' \end{bmatrix} = U(\theta_i) \begin{bmatrix} \alpha_i \\ \beta_i \end{bmatrix} = \begin{bmatrix} \cos(\theta_i) & -\sin(\theta_i) \\ \sin(\theta_i) & \cos(\theta_i) \end{bmatrix} \begin{bmatrix} \alpha_i \\ \beta_i \end{bmatrix} \tag{15}$$

where (α_i', β_i') is the updated probability amplitude of the i-th qubit and θ_i is the rotation angle of each qubit. Because the probability amplitude can be updated on continuous arcs with different rotation angles, QGA also has a better performance in continuous space search.

In addition, the quantum representation cannot be evaluated directly and it should be converted to a binary representation or a real number representation in act of observation for evaluation when applied in practice. The corresponding binary representation or a real number representation is also called the chromosome coding. The observation function can be defined as $f(\alpha_i, \beta_i)$.

Convergence can be obtained with the qubit representation. In the act of observing the quantum states, the chromosome will be collapsed to a certain state. As $|\alpha_i|^2$ and $|\beta_i|^2$ approaches to 1 or 0, the quantum chromosome converges to a single state and the diversity disappears gradually.

B. IMPROVED QUANTUM GENETIC ALGORITHM

Although QGA has good performance and characteristics, most QGAs use a binary chromosome coding method or a real chromosome number coding method, which has problems in some scenes such as complex decoding. What's more, binary chromosome coding or real number chromosome coding can't effectively adapt to task scheduling model with a mixture of multiple decision variables proposed in this paper. So an improved quantum genetic algorithm (IQGA) is proposed based on hybrid chromosome coding of binary and real numbers. Based on the hybrid chromosome coding, the solution space of task scheduling model is mapped into the quantum space. The binary part and the real number part are updated respectively, so the decision variables in the task scheduling model are measured by different observation functions to realize the parallel search.

1) HYBRID CHROMOSOME CODING

As described in Section II, the decision-making of the task scheduling problem can be divided into three parts: first, whether the task is selected to be executed; secondly, if the task is selected to be executed, which time window is selected from its time windows; and thirdly, when to image within the selected time window. So the scheduling strategy of the tasks can be represented as

$$S = \{(x_1, y_1, t_1), \cdots, (x_i, y_i, t_i), \cdots, (x_N, y_N, t_N)\} \quad (16)$$

where x_i, y_i denote the decision variables of task selection, time window selection which are discrete variables, respectively. t_i denotes the decision variables of imaging start time selection which is a continuous variable.

In this paper, we propose a hybrid chromosome coding scheme combined with the binary part and real number part. The coding scheme can be represented as

$$X = \{(u_1, w_1), \cdots, (u_i, w_i), \cdots, (u_N, w_N)\} \quad (17)$$

$$w_i = y_i + z_i, y_i \in \{1, \cdots, M\}, \quad z_i \in [0, 1] \quad (18)$$

where X represents a hybrid chromosome coding scheme for the imaging tasks. (u_i, w_i) represents the solution of the i-th task. u_i is a binary number, which $u_i = 0$ denotes the i-th task is selected to be executed, otherwise not. w_i is a real number that the integer part y_i represents the selection of the task time window, while the decimal part z_i represents the sliding proportion of the imaging start moment within the selected time window. For instance, 0.2 here means the imaging start moment delayed by 20 percent of the time window duration.

The binary part and the real number part of the hybrid chromosome coding scheme can be updated in the quantum space respectively, which means the decision variables in the task scheduling model can be parallel searching in the discrete and continuous domains. Moreover, the coding length of a hybrid coding scheme is only related to the number of tasks and has nothing to do with the number of radars and the number of time windows, which helps to improve the efficiency when the number of radars is large. So compared to single binary or integer chromosome coding methods, the coding structure of a hybrid chromosome coding scheme is practical and efficient.

2) QUANTUM PROBABILITY AMPLITUDE AND OBSERVATION FUNCTIONS

In QGA, the evolution of chromosomes is performed in quantum space. In this paper, the quantum probability amplitude of a hybrid chromosome can be divided into two parts: the binary part and the real number part.

The quantum probability amplitude of a binary part is defined as

$$\begin{aligned} B &= \begin{pmatrix} \alpha_{b1}^t \\ \beta_{b1}^t \end{pmatrix}, \cdots, \begin{pmatrix} \alpha_{bi}^t \\ \beta_{bi}^t \end{pmatrix}, \cdots, \begin{pmatrix} \alpha_{bN}^t \\ \beta_{bN}^t \end{pmatrix} \\ &= \begin{pmatrix} \cos(\theta_{b1}^t) \\ \sin(\theta_{b1}^t) \end{pmatrix}, \cdots, \begin{pmatrix} \cos(\theta_{bi}^t) \\ \sin(\theta_{bi}^t) \end{pmatrix}, \cdots, \begin{pmatrix} \cos(\theta_{bN}^t) \\ \sin(\theta_{bN}^t) \end{pmatrix} \end{aligned} \quad (19)$$

The corresponding observation function is defined as

$$u_i = \begin{cases} 0, & \left|\alpha_{bi}^t\right|^2 > \alpha_0 \\ 1, & \left|\alpha_{bi}^t\right|^2 \le \alpha_0 \end{cases} \quad (20)$$

where α_0 is a threshold constant, usually $\alpha_0 = sqrt(2)/2$.

Thus the decision variable of task selection can be obtained by decoding the binary part of the hybrid chromosome coding scheme as $x_i = u_i$.

The quantum probability amplitude of the real number part is defined as

$$\begin{aligned} R &= \begin{pmatrix} \alpha_{r1}^t \\ \beta_{r1}^t \end{pmatrix}, \cdots, \begin{pmatrix} \alpha_{ri}^t \\ \beta_{ri}^t \end{pmatrix}, \cdots, \begin{pmatrix} \alpha_{rN}^t \\ \beta_{rN}^t \end{pmatrix} \\ &= \begin{pmatrix} \cos(\theta_{r1}^t) \\ \sin(\theta_{r1}^t) \end{pmatrix}, \cdots, \begin{pmatrix} \cos(\theta_{ri}^t) \\ \sin(\theta_{ri}^t) \end{pmatrix}, \cdots, \begin{pmatrix} \cos(\theta_{rN}^t) \\ \sin(\theta_{rN}^t) \end{pmatrix} \end{aligned} \quad (21)$$

The corresponding observation function is defined as

$$w_i = \left|\alpha_{ri}^t\right|^2 \cdot M \quad (22)$$

Then the value of the time window selection variable and the value of the imaging time variable can be obtained as

$$\begin{aligned} y_i &= \lfloor w_i \rfloor \\ z_i &= w_i - y_i \\ t_i &= (1 - z_i) \cdot t_{i,k}^s + z_i \cdot (t_{i,k}^e - T_{di}) \end{aligned} \quad (23)$$

where $t_{i,k}^s, t_{i,k}^e$ represent the start time and terminal time of the k-th time window of the i-th target, T_{di} represents the shortest imaging time of the i-th target and k denotes the selected time window. The symbol $\lfloor\rfloor$ represents round toward minus infinity.

3) INDIVIDUAL UPDATE STRATEGY

In the QGA parent generations create the next generation through the rotation operation based on quantum-gate. The size and direction of the rotation angle need to be obtained through a lookup table.

The quantum-gate $U(\theta_i)$ is a function of $\theta_i = s(\alpha_i, \beta_i) \cdot \Delta\theta_i$ where $s(\alpha_i, \beta_i)$ is the sign of θ_i that determines the direction and $\Delta\theta_i$ is the magnitude of rotation angle. The lookup table

TABLE 1. Lookup table for rotation angle.

r_i	b_i	$f(r)<f(b)$	$\Delta\theta_i$	$s(\alpha_i,\beta_i)$			
				$\alpha_i\beta_i>0$	$\alpha_i\beta_i<0$	$\alpha_i=0$	$\beta_i=0$
0	0	False	0	0	0	0	0
0	0	True	0	0	0	0	0
0	1	False	0	0	0	0	0
0	1	True	0.05π	-1	+1	±1	0
1	0	False	0.01π	-1	+1	±1	0
1	0	True	0.025π	+1	-1	0	±1
1	1	False	0.005π	+1	-1	0	±1
1	1	True	0.025π	+1	-1	0	±1

of $\Delta\theta_i$ is shown in Table 1, where $f(\cdot)$ is the fitness function (i.e. the objective function of the proposed model), b_i and r_i are the i-th bit of the best solution b and a current solution r, respectively. Thus the use of quantum-gate rotation is to emphasize the searching direction toward the best solution.

Based on the rotation of quantum-gate, each chromosome is updated toward the current optimal chromosome. If the current optimal chromosome is a local optimal solution, it may lead to precocity. In order to enhance the diversity of the population and reduce the possibility of precocity, the quantum NOT gate is considered to update the population by disturbance. Specifically, randomly selects several chromosomes according to the probability of mutation, and then randomly selects partial gene positions of the selected chromosomes, and applies a quantum NOT operation to these gene positions. The definition of the quantum NOT gate formula is defined as

$$\begin{pmatrix}\alpha_i'\\ \beta_i'\end{pmatrix}=\begin{pmatrix}0 & 1\\ 1 & 0\end{pmatrix}\cdot\begin{pmatrix}\alpha_i\\ \beta_i\end{pmatrix} \tag{24}$$

In view of the above analysis, an improved Quantum Genetic Algorithm (IQGA) is proposed to tackle the multi-target ISAR imaging task scheduling problem. The concrete steps of the IQGA in detail is as follows:

Step 1): Let generation $t = 0$ and randomly generate an initial population $Q(t) = \{q_1^t, q_2^t, \cdots, q_L^t\}$, where L is the size of the population, and q_j^t denotes the j-th individual (n-qubits chromosome) in the t-th generation.

Step 2): Make a set of solutions $P(t)$ by observing $Q(t)$ states, where $P(t) = \{X_1^t, X_2^t, \cdots, X_L^t\}$ and the observation function is illustrated in by (20) and (22).

Step 3): Evaluate the fitness of the solution $P(t)$, perform trimming operation, and store the best solution b.

Step 4): If a stopping condition is satisfied, then output the result; otherwise, go on to the following steps.

Step 5): Update the population to generate $Q(t+1)$ by perform the rotation Quantum-gate and the Quantum-Not gate.

Step 6): Let $t = t + 1$ and go back to Step 2).

IV. EXPERIMENTS

In order to verify the validity of the task scheduling model and the effectiveness of the proposed improved Quantum Genetic Algorithm, some simulation experiments are performed. Two reconnaissance scenes with different scale are chosen as the task scheduling problem for multi-target ISAR imaging in radar network. The small-scale scene is constituted by 3 radars and 10 targets, while the large-scale scene is constituted by 4 radars and 12 targets. The geometry of the radars and targets of the two scenes are illustrated in Fig.4 and Fig.5 respectively.

TABLE 2. The prior information in small-scale scene.

Target	Coordinate (km)	Speed (m/s)	RCS(m^2)
Target 1	(220, 240, 15)	(-500,100,0)	6
Target 2	(240, 180, 16)	(-510,120,0)	2
Target 3	(220, 190, 14)	(-520,120,0)	6
Target 4	(250, 210, 15)	(-500,80,0)	6
Target 5	(240, 210, 16)	(-520,90,0)	6
Target 6	(210, -190, 17)	(-30,420,0)	2
Target 7	(200, -200, 16)	(-40,460,0)	2
Target 8	(200, -100, 14)	(320,210,0)	6
Target 9	(190, -140, 15)	(320,220,0)	6
Target 10	(180, -150, 16)	(220,310,0)	2

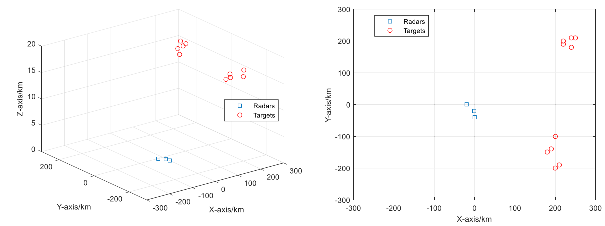

(a) (b)

FIGURE 4. Geometry of the radars and targets in small-scale scene. (a) Three-dimensional perspective. (b) Top view.

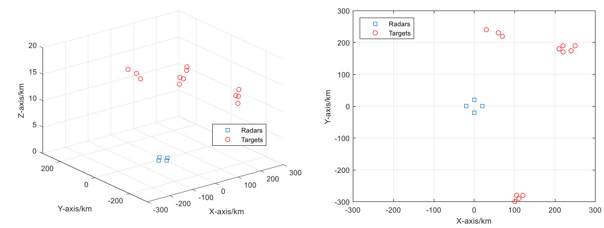

(a) (b)

FIGURE 5. Geometry of the radars and targets in large-scale scene. (a) Three-dimensional perspective. (b) Top view.

In practice, the target characteristics such as the speed, the coordinate can be estimated by conventional tracking algorithms, let us suppose the target characteristics as prior information, then the priority can be evaluated according to [15]. The prior information is illustrated in Table 2 and Table 3, corresponding to the two scenes of different scale. For the targets which have different RCS, the required imaging resolutions are different and the target with larger RCS requires lower resolution. Thus, in this paper, the required

TABLE 3. **The prior information in large-scale scene.**

Target	Coordinate (km)	Speed (m/s)	RCS(m^2)
Target 1	(220, 170, 10)	(-400, 90, 0)	6
Target 2	(210, 180, 9)	(-410, 80, 0)	2
Target 3	(220, 190, 10)	(-420, 90, 0)	2
Target 4	(250, 190, 11)	(-400, 80, 0)	6
Target 5	(240, 175, 12)	(-420, 90, 0)	6
Target 6	(100, -300, 14)	(-320,70,0)	2
Target 7	(110, -290, 15)	(-330,120,0)	6
Target 8	(120, -280, 16)	(-340,30,0)	2
Target 9	(105, -280, 15)	(-330, 110, 0)	6
Target 10	(30, 240, 13)	(240, -90, 0)	6
Target 11	(60, 230, 12)	(235, -80, 0)	2
Target 12	(70, 220, 11)	(250, -95, 0)	6

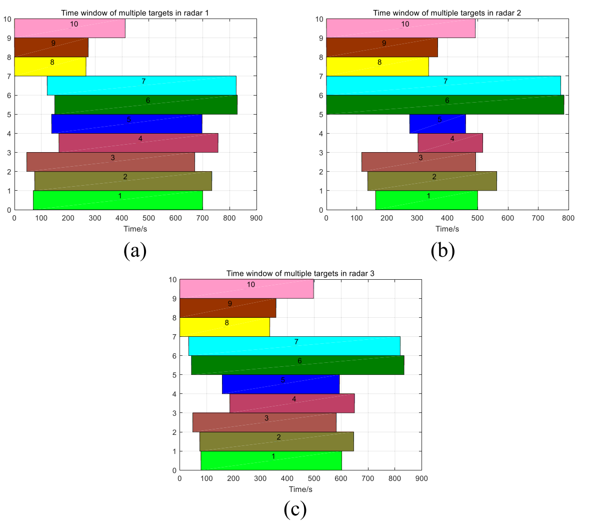

FIGURE 6. **Gantt charts of the imaging time window in small scale scene. (a) The imaging time window of targets if observed by radar 1. (b) The imaging time window of targets if observed by radar 2. (c) The imaging time window of targets if observed by radar 3.**

imaging resolutions for targets with large and small RCS are 0.8m and 0.5m respectively.

Suppose each radar has the same technical parameters such as the radar transmitted power $P_t = 500$kW, the antenna gain $G = 40$dB, the carrier frequency of radar signal $f_c = 10$GHz, the noise figure $F_n = 3$dB and the minimum output SNR for detecting signal $(S/N)_{\min} = 8$dB. Therefore, the maximum radar range can be evaluated by (2) and the imaging time windows can be calculated by (3) and (4).

A Gantt chart is used to describe the imaging time window. The horizontal axis and the vertical axis represent the time and the number of the target, respectively. Different colors are used to distinguish the targets, and the number on the time windows represents the corresponding target. The imaging time windows of targets are illustrated in Fig. 6 and Fig. 7 of two scenes. Take small scale scene for example, In Fig. 6 we can see the imaging time window is different even for the same target when imaged by different radars. The imaging start time must be within the time window and the imaging task must finish within the time window.

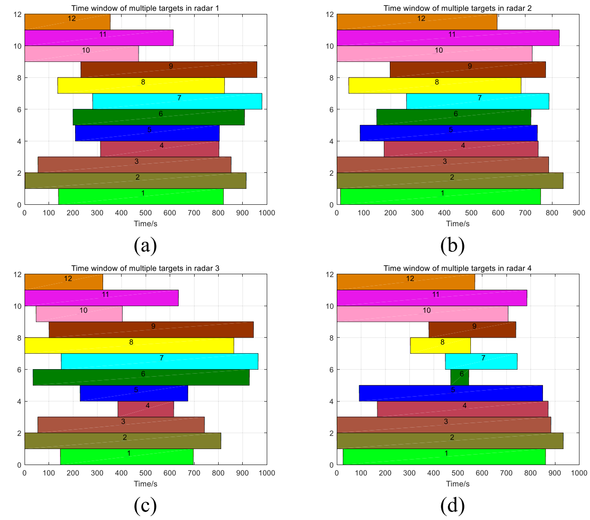

FIGURE 7. **Gantt charts of the imaging time window in large scale scene. (a) The imaging time window of targets if observed by radar 1. (b) The imaging time window of targets if observed by radar 2. (c) The imaging time window of targets if observed by radar 3. (d) The imaging time window of targets if observed by radar 4.**

TABLE 4. **The optimal strategy profile.**

Parameter	Value
Population size	200
Mutation probability	0.05
Maximum iterations	200

The imaging time, which affects the utilization of radar resources, is time sensitive and largely determined by the imaging start time. According to the prior information in two reconnaissance scenes, all imaging task times of multiple targets are calculated, and then the imaging task scheduling models in small-scale and large scale radar network are constructed. Suppose the adjustment factors are $w_1 = 0.5$ and $w_2 = 0.5$. The proposed algorithm IQGA is used to solve the optimization problem by averaging 200 independent Monte Carlo experiments in each scene. The parameters in IQGA are set as illustrated in Table 4.

Therefore, based on the proposed algorithm IQGA, the optimal task scheduling strategy can be obtained, as illustrated in Table 5 and Fig. 8.

The Gantt charts are used to describe the optimal task scheduling strategy in Fig. 8. The horizontal axis and the vertical axis represent the time and the serial number of the radar, respectively. The targets in the same color are allocated to the same radar. As shown in Fig. 8, the rectangular time box and the left edge of the rectangular time box indicate the imaging time and the imaging start time, respectively. Under the limits of the time window, less radar resources are used to perform the multi-target imaging task. Therefore the radar resources utilization for multi-target imaging is improved

TABLE 5. The optimal task scheduling profile.

Case	Radar	Strategy profile
Small-scale scene	Radar 1	Target 5，Target 6，Target 8
	Radar 2	Target 1，Target 9，Target 10
	Radar 3	Target 2，Target 3，Target 4，Target 7
Large-scale scene	Radar 1	Target 3, Target 7
	Radar 2	Target 10, Target 4, Target 11, Target 5
	Radar 3	Target 12, Target 8, Target 6, Target 2, Target 9
	Radar 4	Target 1

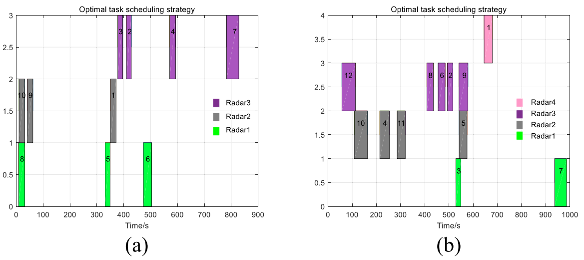

FIGURE 8. Gantt chart of the optimal task scheduling strategy. (a) Small scale scene. (b) Large scale scene.

by optimizing the task scheduling strategy at suitable time in radar network and the multi-target ISAR imaging task is completed under the image quality requirement. More resources remained can be used for other important tasks such as searching and tracking.

Furthermore, according to the task scheduling strategy of small-scale scene, let the radars observe the corresponding targets at the suitable time and calculate the imaging results by the conventional RD algorithm respectively. The imaging results of the representative targets which contain Target 3 and Target 6 are illustrated in Fig. 9. From the results we can see that the imaging resolution can be achieved within the imaging time window.

The conventional GA often use binary coding structure to tackle the optimization problem, which objectively discretize the solution space, especially the imaging start time selection. The quality of search solution is influenced by different discrete granularity. Based on hybrid coding structure of binary and real numbers, the solution space of the multi-target task scheduling problem with a mixture of multiple decision variables can be mapped into the quantum space, then QGA is introduced to solve the optimization problem. It can be seen from the experiments that proposed IQGA effectively solves the task scheduling problem for multi-target ISAR imaging in radar network.

In [14], for the first time, a multi-target imaging task allocation method in radar network has been proposed. Therefore some experiments are performed to contrast the efficiency of the proposed IQGA algorithm and the convex optimization algorithm in [14]. The conventional Range-Doppler (RD) algorithm are used to conduct the ISAR image and the algorithms are executed in two scenes to yield the following results as illustrated in Table 6.

TABLE 6. Parameters of performance metrics.

RSR	Small-Scale Scene	Large-Scale Scene
Algorithm in [14]	65.85%	49.1%
Proposed algorithm	77.16%	55.84%

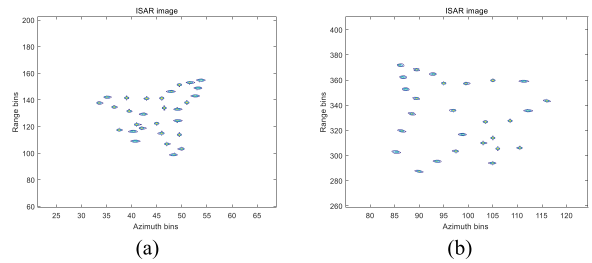

FIGURE 9. The imaging results of the representative targets in small scale scene. (a) The imaging result of target 3. (b) The imaging result of target 6.

It is observed that the proposed method can improve the radar resource utilization while obtaining the required ISAR image.

According to the above experiments, we can see that the proposed method has the ability to acquire an effective strategy profile to achieve the multi-target imaging task at suitable time in radar network under the image quality requirement, which improves the working efficiency of the radar network significantly.

V. CONCLUSION

In this paper, we studied an optimization problem of task scheduling for multi-target ISAR imaging in radar network. Under restriction of limited radar resources, we devoted to improve the radar resources utilization through optimizing the task scheduling scheme. Image resolution is chosen as a metric to evaluate the imaging task. The relationship between the imaging resolution and task time is studied firstly, and the imaging task is time sensitive due to the imaging start moment. Then the task scheduling optimization model with time window constrains has been constructed. An improved Quantum Genetic Algorithm (IQGA) is proposed to solve the problem. Finally, the proposed imaging task schedule optimization method is applied to two scenarios. The experimental results showed that our method can design task scheduling strategy, which is capable to improve the resource utilization the radar network while the requirement of imaging resolution is fulfilled. We notice that only time resource is considered in this paper, while some other kinds of radar resources such as energy and aperture are also important. We also notice that only Conventional RD imaging algorithm is considered in this paper, while some other imaging algorithms such as CS-based sparse aperture ISAR imaging algorithms are also important. In our future works, the proposed model can be extended with consideration of more other kinds of radar resources and imaging algorithms.

REFERENCES

[1] M. A. Richards, *Fundamentals of Radar Signal Processing*, 2nd. New York, NY, USA: McGraw-Hill, 2014.

[2] Y. Zhou, Z. Lei, H. Wang, and M. Xing, "Performance analysis on ISAR imaging of space targets," *J. Radars*, vol. 6, no. 1, pp. 17–24, Jan. 2017, doi: 10.12000/JR16136.

[3] X. Bai, F. Zhou, M. Xing, and Z. Bao, "High-resolution radar imaging of air targets from sparse azimuth data," *IEEE Trans. Aerosp. Electron. Syst.*, vol. 48, no. 2, pp. 1643–1655, Apr. 2012.

[4] J.-F. Huang, G.-Y. Chang, and J.-X. Huang, "Anti-jamming rendezvous scheme for cognitive radio networks," *IEEE Trans. Mobile Comput.*, vol. 16, no. 3, pp. 648–661, Mar. 2017.

[5] Y.-J. Chen, Q. Zhang, Y. Luo, and Y.-A. Chen, "Measurement matrix optimization for ISAR sparse imaging based on genetic algorithm," *IEEE Geosci. Remote Sens. Lett.*, vol. 13, no. 12, pp. 1875–1879, Dec. 2016.

[6] Y. Yang, T. Zhang, W. Yi, L. Kong, X. Li, and X. Yang, "Multi-static radar power allocation for multi-stage stochastic task of missile interception," *IET Radar, Sonar Navigat.*, vol. 12, no. 5, pp. 540–548, May 2018.

[7] T. Zhang, J. Liang, Y. Yang, G. Cui, L. Kong, and X. Yang, "Antenna deployment method for multistatic radar under the situation of multiple regions for interference," *Signal Process.*, vol. 143, pp. 292–297, Feb. 2018.

[8] J. Yan, H. Liu, B. Jiu, and Z. Bao, "Power allocation algorithm for target tracking in unmodulated continuous wave radar network," *IEEE Sensors J.*, vol. 15, no. 2, pp. 1098–1108, Feb. 2015.

[9] T. Tian, T. Zhang, and L. Kong, "Timeliness constrained task scheduling for multifunction radar network," *IEEE Sensors J.*, vol. 19, no. 2, pp. 525–534, Jan. 2019.

[10] Y. Yang, W. Yi, T. Zhang, G. Cui, L. Kong, X. Yang, and J. Yang, "Fast optimal antenna placement for distributed MIMO radar with surveillance performance," *IEEE Signal Process. Lett.*, vol. 22, no. 11, pp. 1955–1959, Nov. 2015.

[11] P. Chen, C. Qi, and L. Wu, "Antenna placement optimisation for compressed sensing-based distributed MIMO radar," *IET Radar, Sonar Navigat.*, vol. 11, no. 2, pp. 285–293, 2016.

[12] W.-J. Chen and R. M. Narayanan, "Antenna placement for minimizing target localization error in UWB MIMO noise radar," *IEEE Antennas Wireless Propag. Lett.*, vol. 10, pp. 135–138, 2011.

[13] D.-S. Jang, H.-L. Choi, and J.-E. Roh, "A time-window-based task scheduling approach for multi-function phased array radars," in *Proc. 11th Int. Conf. Control, Automat. Syst.*, Oct. 2011, pp. 1250–1255.

[14] X.-W. Liu, Q. Zhang, Y.-C. Chen, L.-H. Su, and Y.-J. Chen, "Task allocation optimization for multi-target ISAR imaging in radar network," *IEEE Sensors J.*, vol. 18, no. 1, pp. 122–132, Jan. 2018.

[15] Y. Chen, Q. Zhang, N. Yuan, Y. Luo, and H. Lou, "An adaptive ISAR-Imaging-Considered task scheduling algorithm for multi-function phased array radars," *IEEE Trans. Signal Process.*, vol. 63, no. 19, pp. 5096–5110, Oct. 2015.

[16] M. Xie, W. Yi, T. Kirubarajan, and L. Kong, "Joint node selection and power allocation strategy for multitarget tracking in decentralized radar networks," *IEEE Trans. Signal Process.*, vol. 66, no. 3, pp. 729–743, Feb. 2018.

[17] M. Ben Kilani, G. Gagnon, and F. Gagnon, "Multistatic radar placement optimization for cooperative radar-communication systems," *IEEE Commun. Lett.*, vol. 22, no. 8, pp. 1576–1579, Aug. 2018.

[18] J. Yan, H. Liu, W. Pu, H. Liu, Z. Liu, and Z. Bao, "Joint threshold adjustment and power allocation for cognitive target tracking in asynchronous radar network," *IEEE Trans. Signal Process.*, vol. 65, no. 12, pp. 3094–3106, Jun. 2017.

[19] J. Yan, W. Pu, S. Zhou, H. Liu, and Z. Bao, "Collaborative detection and power allocation framework for target tracking in multiple radar system," *Inf. Fusion*, vol. 55, pp. 173–183, Mar. 2020.

[20] K.-H. Han and J.-H. Kim, "Genetic quantum algorithm and its application to combinatorial optimization problem," in *Proc. Congr. Evol. Comput.*, Istanbul, Turkey, Jul. 2000, pp. 1354–1360.

[21] W. Haijiao, H. Huan, and Y. Zhen, "Scheduling of Agile Satellites Based on an Improved Quantum Genetic Algorithm," *J. Astronaut.*, vol. 39, no. 11, pp. 1266–1274, 2018.

[22] L. Wang, H. Wu, F. Tang, and D.-Z. Zheng, "A hybrid quantum-inspired genetic algorithm for flow shop scheduling," in *Advances in Intelligent Computing* (Lecture Notes in Computer Science), vol. 3645. Berlin, Germany: Springer-Verlag, 2005, pp. 636–644.

[23] K.-H. Han and J.-H. Kim, "Quantum-inspired evolutionary algorithm for a class of combinatorial optimization," *IEEE Trans. Evol. Comput.*, vol. 6, no. 6, pp. 580–593, Dec. 2002.

[24] M. R. Garey and D. S. Johnson, Eds., *Computers and Intractability: 'A Guide to the Theory of NP-Completeness*. San Francisco, CA, USA: Freeman, 1979.

[25] M. Nawaz, E. E. Enscore, and I. Ham, "A heuristic algorithm for the m-machine, n-job flow-shop sequencing problem," *Omega*, vol. 11, no. 1, pp. 91–95, Jan. 1983.

[26] G. X. Zhang, N. Li, and W. D. Jin, "A Novel Quantum Genetic Algorithm and Its Application," *Chin. J. Electron.*, vol. 32, pp. 476–479, Mar. 2004.

[27] L. Wang, F. Tang, and H. Wu, "Hybrid genetic algorithm based on quantum computing for numerical optimization and parameter estimation," *Appl. Math. Comput.*, vol. 171, no. 2, pp. 1141–1156, Dec. 2005.

[28] B.-B. Li and L. Wang, "A hybrid quantum-inspired genetic algorithm for multiobjective flow shop scheduling," *IEEE Trans. Syst., Man Cybern., B (Cybern.)*, vol. 37, no. 3, pp. 576–591, Jun. 2007.